COBEM 2021 26th International Congress of Mechanical Engineering
November 22-26, 2021, Virtual Congress, Brazil

COB-2021-1452
Analysis of process parameters influence on quality performance and energy consumption of resistance spot welding

Carla Ferreira Andrade Cunha
Fábio do Monte Sena
Jefferson de Oliveira Gomes
Instituto Tecnológico de Aeronáutica. Department of Aeronautical and Mechanical Engineering. São José dos Campos, SP, Brazil.
carla@ita.br, sena@ita.br, gomes@ita.br

Abstract. *Resistance spot welding is widely used in the automotive sector. The high production volumes - 2 million in 2020 in Brazil - lead to huge quantities of welds manufactured, since there are 4,000 to 6,000 spot welds in a passenger vehicle. Inspection limitations and few backgrounds of the quality-energy consumption relationship lead the industry to waste and high operational costs. In this regard, this study aims to evaluate quality aspects simultaneously to energy consumption. For this purpose, a design of experiments together with statistical analysis was performed. Spot welds samples were conducted using two CR4 steel sheets with 0.7 mm thickness welded in a low-frequency machine. The influence of the following process parameters: welding current, welding time, and electrode force were investigated. Energy consumption was measured for each sample, subsequently subjected to a tensile-shear test. The factors with the greatest influence on the quality aspects were welding current, time, and the interaction between current and force, responsible for changing the electrical resistance conditions of the system. Energy consumption was influenced by current, time, and its interaction. The result of this work provides to spread good practices for real applications in the industrial environment.*

Keywords: *Resistance Spot Welding; RSW; Energy Consumption; Efficiency; ANOVA*

1. INTRODUCTION

Resistance Spot Welding (RSW) combines two or more thin, overlapping sheets by applying a high electrical current to them through electrodes. It is one of the most important manufacturing processes applied to automotive manufacturing (Colombo et al., 2017). In 2020 around 2 million motor vehicles were manufactured in Brazil (International Organization of Motors Vehicle Manufacturers, 2021). In a typical passenger vehicle, there are between 4,000 and 6,000 spot welds, of which 30% can have a heat input greater than necessary (Uijl, 2015; Williams and Parker, 2004). Therefore, it is estimated that the number of spot welds manufactured in Brazil is in the order of magnitude of 10 billion, in 2020 alone. It is also noted that this considerable number of spot welds is strongly influenced by the difficulty of evaluating their quality. Since quality control in production lines is highly dependable on manual inspection methods, sampling control is very low and generates productivity losses (Boersch et al., 2018).

The key parameters to be correctly set in RSW process are welding current, electrode force, and welding time. According to Zhang and Senkara (2011), the mechanical and metallurgical features of the spot welds may be strongly dependent on the welding parameters. Mechanical properties in spot welding are highly dependable on welding current, which is also consistent with nugget size growth (Afshari, 2013; Kianerski et al., 2014; Pouranvari, 2017; Yuan et al., 2017). Longer welding times have a lower impact on weld spot strength and dimensions, as the nugget growth rate is high only in the few early welding cycles (Moshayedi and Sattari-Far, 2014; Pouranvari et al., 2007, 2011). Electrode force affects the contact electrical resistance of the material being welded. Higher electrode forces improve the interfacial contact between the metal sheets, thus reducing resistance. This parameter may either favor or impair the load-bearing capacity of the spot welds (Afshari, 2013; Rao et al., 2017; Sun et al., 2007; Yuan et al., 2017).

The less energy spent in RSW means a most efficient process in terms of electrical energy consumption. Few studies approach quality and energy consumption together. Venugopal et al. (2009) analyze force's influence on spot welding quality and shows that higher forces allow the use of lower current and time. Hence, the author suggests that higher forces result, indirectly, in less energy consumption. Nie et al. (2018) propose a Finite Elements Method (FEM) to optimize RSW process parameters, which indicates a reduction of 55% in energy consumption.

Literature well knows the effects of RSW parameters in welding nugget quality, regarding its size and tensile-shear test results. However, it lacks studies that better understands how quality is related to electrical energy consumption. Therefore, the objective of this study is to investigate the influence of the three main process parameters on the RSW's quality and energy consumption.

2. MATERIALS AND METHODS

The welds were carried out using a single-phase AC spot-welding machine (Düring Easy Line – CB150 – 85 kVA – 60 Hz). The machine has a manual pneumatic drive, Harms & Wende Ratia 73 controller, and is equipped with a dedicated water cooling system. Welding parameters are configured using the Pegasus platform, software available together with the welding machine that allows actuation on process parameters. Copper electrodes with a face diameter of 6.0 mm standardized according to DIN 44750 were used. The samples were manufactured with two sheets of CR4 galvanized steel, whose chemical composition and mechanical properties are shown in Table 1. They have a thickness of 0.7 mm and were cut to the size of 50 x 30 mm.

Table 1 – Chemical composition and mechanical properties of the base material (CR4 galvanized).

Chemical composition (%wt.)				**Mechanical Properties**	
C (max)	Mn (max)	P (max)	S (max)	Yield Strength (MPa)	Ultimate Tensile Strength (MPa)
0.12	0.60	0.05	0.05	140 (min.)	280 (min.)

To investigate the influence on the quality and energy consumption of the spot weld, a full factorial design with 3 factors and 2 replications was carried out. The first factor, welding current, was used in 4 levels (8 kA, 10 kA, 12 kA, and 14 kA), the second factor, welding time, in 4 levels (8, 12, 16, and 20 cycles), and the last factor, electrode force, in 2 levels (180 kgf and 285 kgf). These values were selected because they represent ranges typically used in the industry. The experiment was carried out by three operators with previous experience. In addition, the samples were welded in random order.

To carry out the mechanical characterization, the tensile-shear test was carried out in a universal testing machine model Instron 5500R, with a load cell of 30 kN. A strain rate of 10 mm/min, suitable for the test, was used. Data were post-processed in an Excel spreadsheet to acquire the values of Maximum Force and Absorbed Energy. The first is characterized by the maximum peak that the weld joint can withstand before it fails and the second by the area under the curve before a fracture occurs. The values of Maximum Force (kN) and Absorbed Energy (J) were used to perform the statistical analyses.

Energy consumption was measured using an energy analyzer Fluke 1738. The measurements were obtained from the primary circuit of the welding machine, with a two-phase characteristic consisting of 220V in each phase. The equipment extracts the voltage (V) and current (A) values for each weld, returning the energy consumption (W). The data generated therefore represent the amount of energy that the welding machine extracts from the electrical network for the manufacture of spot welds. The electrical energy associated with the consumption of compressed air, for the action of the electrodes, was not considered in this study.

The analysis of the results was performed in R Studio version 1.1.453, an open-source software application for graphical and statistical analysis.

3. RESULTS AND DISCUSSIONS

The results include the analyzes discussed for the mechanical strength of the joints, and for the resulting energy consumption.

3.1 Mechanical Resistance

The structural integrity of the joints is assessed by the results of the tensile-shear test. Thus, in Figures 1 and 2, the isolated effects of the main factors under analysis on Maximum Force (F_{max}) and Absorbed Energy (En_{abs}) are shown. Graphical analysis shows similar behavior for both responses. It is noted that the increase in the magnitude of the electric current, increases both F_{max} and En_{abs}. The welding time also increases the mechanical resistance of the joint, although there is an indication of stabilization in these values for longer times. Regarding electrode force, there is little or irrelevant influence on the responses.

The results show the importance of the heat generated in the formation of the weld spot. The greater the magnitude of thermal energy introduced into the process, the stronger the weld joint. This energy is governed by the equation that expresses the Joule effect (Equation 1):

$$Q = r \int_{t_i}^{t_f} I^2 R_T dt \qquad (1)$$

where Q is the total thermal energy in Joules (J), I is the welding current in amperes (A), R_T is the electrical resistance in Ohms (Ω), r is the thermal efficiency of the process considering heat losses by radiation and convection, t is the time in seconds (s), where t_i and t_f are the start and end times, respectively.

Equation 1 highlights why the current and time parameters show such an influence on the process. After evaluating the main factors disconnectedly, the interactions between them are analyzed, as shown in Figures 3 and 4.

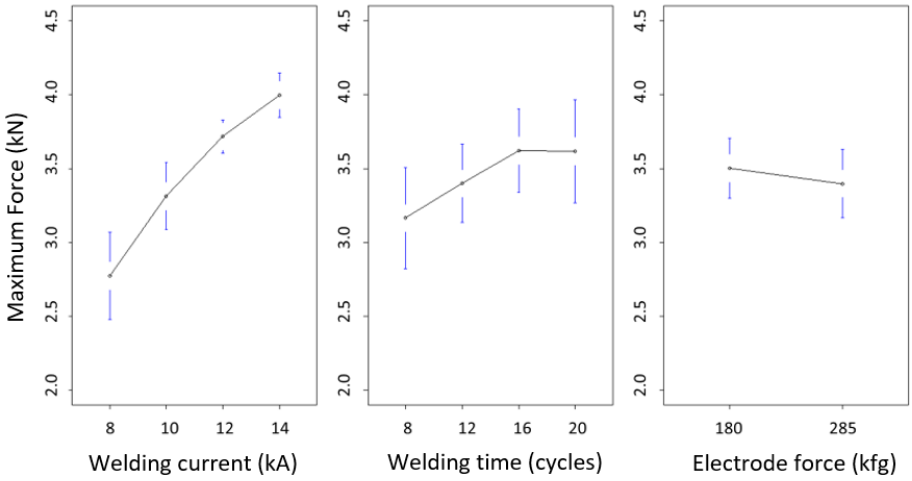

Figure 1 – Effect of factors on Maximum Force (kN).

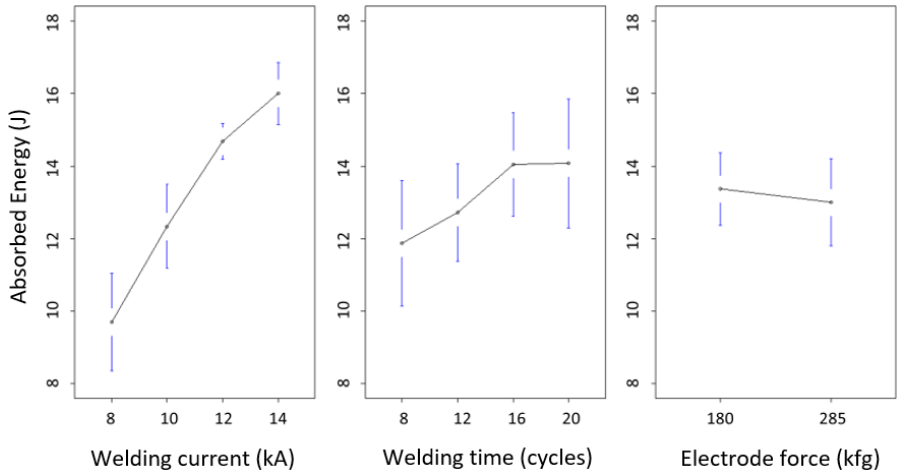

Figure 2 – Effect of factors on Energy Absorbed (J).

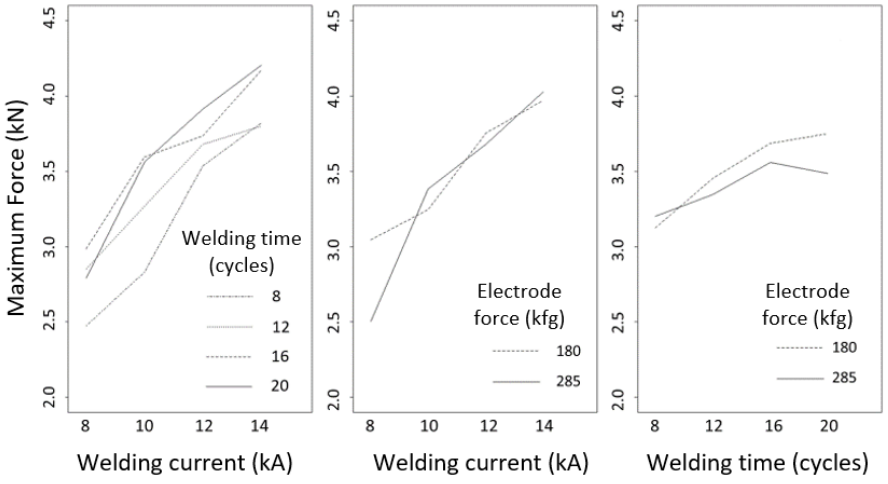

Figure 3 – Effect of the interaction between factors on the Maximum Force (kN).

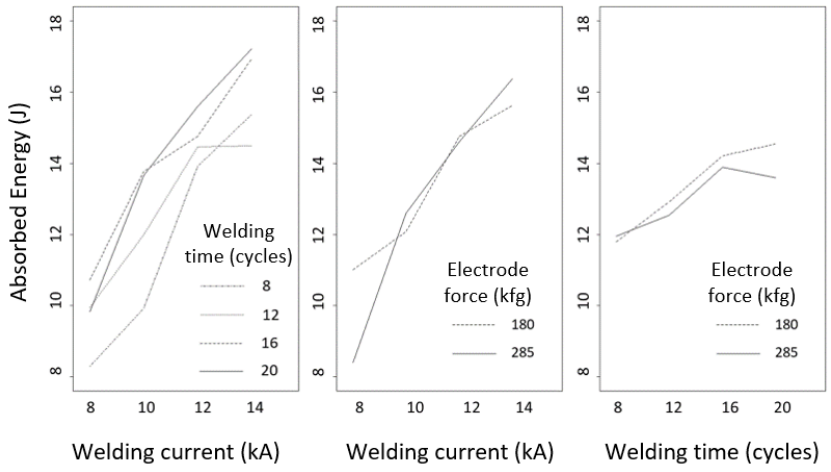

Figure 4 – Effect of the interaction between factors on Energy absorbed (J).

As for the main factors, the behaviors of the interaction graphs are also similar. The increase in heat input, resulting from the additions in current and time, generate more resistant joints. Therefore, the fact that there was probably no metallurgical change in the material, which could promote an unexpected failure behavior, is configured. The hypotheses raised by the graphical analysis can be validated by the Analysis of Variance (ANOVA). For both tensile-shear test responses, the most influential parameters are current and time. In the case of F_{max}, the current showed the most influential effect, followed by time and the interaction between current and force, with respective confidence intervals of 99.9%, 99%, and 95%. As for the En_{abs}, both current and time factors were very influential, followed by the interaction of current and force. Confidence intervals were 99.9%, 99.9% and 95%, respectively. These results are supported by the residue analysis. The Shapiro Wilk test reinforces that no systematic error was present. The p-value for the Maximum Force model was 0.1189 and for the Absorbed Energy, 0.08325, greater than the adopted criterion of 0.05 significance.

These results confirm the relevance of heat input as a means of ensuring the structural integrity of spot-welded joints. It was also possible to assess that the interaction between current and force also influences the responses. The force could influence the electrical resistance especially at the interfaces: cover to plate, and plate to plate. Thus, the passage of electric current from one surface to the other is facilitated, or hindered, by the compressive action of the electrodes. Therefore, there is an important contribution to the heat generated in the system from this phenomenon, which cannot be neglected.

Finally, a linear statistical model for each of the responses is proposed. Through it, it is possible to predict the behavior of mechanical strength within the region characterized experimentally. The linear model adjusted for F_{max} is given in Figure 5, and for the Absorbed Energy, in Figure 6.

```
Call:
lm.default(formula = FMAX ~ A * B * C + I(B^2) + I(A * B^2) +
    I(A^2 * B))

Residuals:
     Min       1Q   Median       3Q      Max
-0.75630 -0.15687 -0.00792  0.19813  0.57291

Coefficients:
              Estimate Std. Error t value Pr(>|t|)
(Intercept) -8.9358100  3.7200988  -2.402  0.01984 *
A            0.9618162  0.3314127   2.902  0.00539 **
B            1.1198175  0.4075668   2.748  0.00819 **
C            2.3169500  1.2880934   1.799  0.07775 .
I(B^2)      -0.0241719  0.0122486  -1.973  0.05367 .
I(A * B^2)   0.0018574  0.0010912   1.702  0.09458 .
I(A^2 * B)  -0.0012052  0.0006641  -1.815  0.07522 .
A:B         -0.0694470  0.0385316  -1.802  0.07718 .
A:C         -0.1870750  0.1147525  -1.630  0.10898
B:C         -0.2359250  0.0876437  -2.692  0.00949 **
A:B:C        0.0190812  0.0078079   2.444  0.01789 *
---
Signif. codes:  0 ‘***’ 0.001 ‘**’ 0.01 ‘*’ 0.05 ‘.’ 0.1 ‘ ’ 1

Residual standard error: 0.3123 on 53 degrees of freedom
Multiple R-squared:  0.7729,    Adjusted R-squared:  0.7301
F-statistic: 18.04 on 10 and 53 DF,  p-value: 9.516e-14
```

Figure 5 – Linear model proposed for the Maximum Force (kN).

```
Call:
lm.default(formula = EABS ~ A * B * C + I(B^2) + I(A * B^2) +
    I(A^2 * B))

Residuals:
    Min      1Q  Median      3Q     Max
-3.5411 -0.7142  0.0690  0.9005  2.6165

Coefficients:
              Estimate Std. Error t value Pr(>|t|)
(Intercept) -49.873355  17.619857  -2.831  0.00655 **
A             5.112586   1.569702   3.257  0.00197 **
B             5.876527   1.930397   3.044  0.00363 **
C            11.201100   6.100919   1.836  0.07197 .
I(B^2)       -0.129742   0.058014  -2.236  0.02956 *
I(A * B^2)    0.010631   0.005168   2.057  0.04463 *
I(A^2 * B)   -0.006051   0.003145  -1.924  0.05975 .
A:B          -0.397167   0.182501  -2.176  0.03401 *
A:C          -0.947600   0.543513  -1.743  0.08705 .
B:C          -1.195025   0.415115  -2.879  0.00575 **
A:B:C         0.101181   0.036981   2.736  0.00844 **
---
Signif. codes:  0 ‘***’ 0.001 ‘**’ 0.01 ‘*’ 0.05 ‘.’ 0.1 ‘ ’ 1

Residual standard error: 1.479 on 53 degrees of freedom
Multiple R-squared:  0.8022,    Adjusted R-squared:  0.7649
F-statistic:  21.5 on 10 and 53 DF,  p-value: 2.814e-15
```

Figure 6 – Proposed Linear Model for Energy Absorbed (J).

In both responses, it was possible to obtain linear models with a strong correlation. In the case of Maximum Force, this is represented by an R^2 of 0.77, while for Absorbed Energy R^2 value is 0.80. Residual analysis for linear models was conducted in the same way as for ANOVA, indicating that there is no systematic error in the model construction. With this, it is possible to trace a response surface that represents the linear model obtained by the experiment. Response surfaces are presented in Figures 7 and 8.

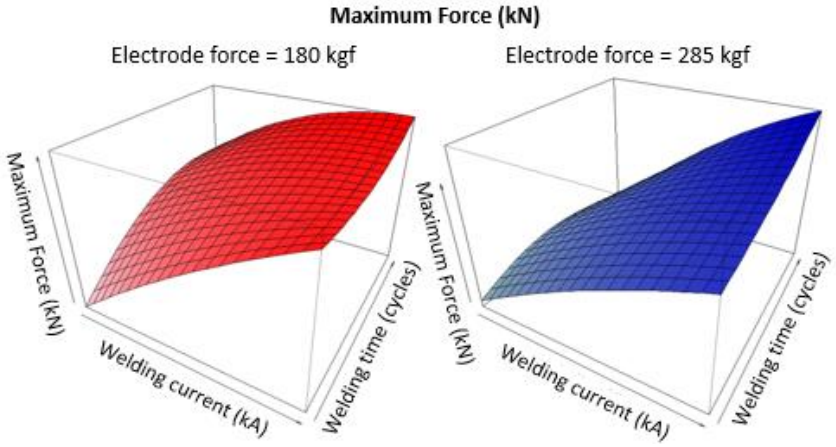

Figure 7 – Response surface for the linear model of Maximum Force (kN).

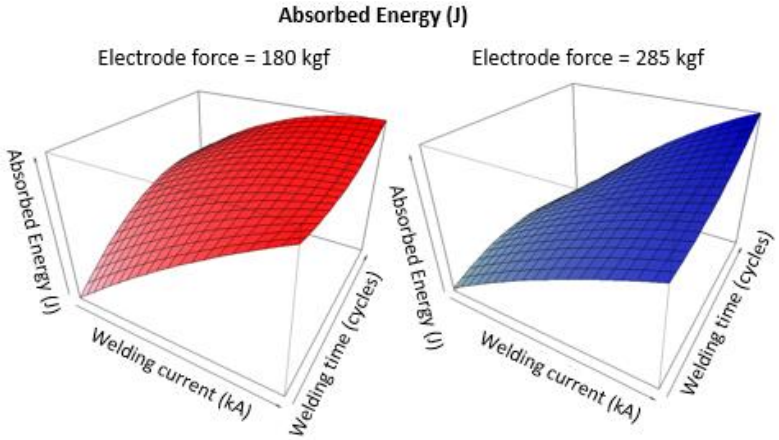

Figure 8 – Response surface for the linear model of energy absorbed (J).

The models' contour curves are presented in Figures 9 and 10, they demonstrate the growth of the responses when more energy is inserted into the system. This is given both by increasing the magnitude of the electrical current, and by allowing it to pass for longer (increased welding time). For the lowest force (180 kgf) there is a slight stagnation in resistance gains in the largest thermal inputs. On the other hand, at the upper force level (285 kgf), it was possible to reach higher resistance values. Furthermore, it is possible to observe the reduction of F_{max} and $En_{abs}$when the electrode force is increased. This highlights the fact that greater power leads to a reduction in the total heat generated, as it facilitates the passage of electric current and, therefore, the amount of heat generated is reduced. Thus, greater thermal inputs are an effective measure to ensure the good mechanical performance of spot-welded joints. The counterpart, however, is the expense associated with the consumption of electricity.

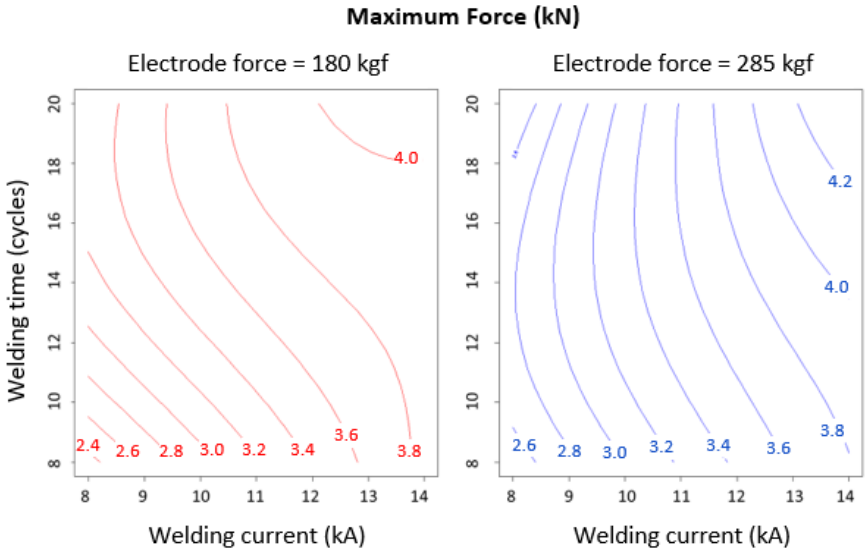

Figure 9 – Contour curves of the response of the linear model of Maximum Force (kN).

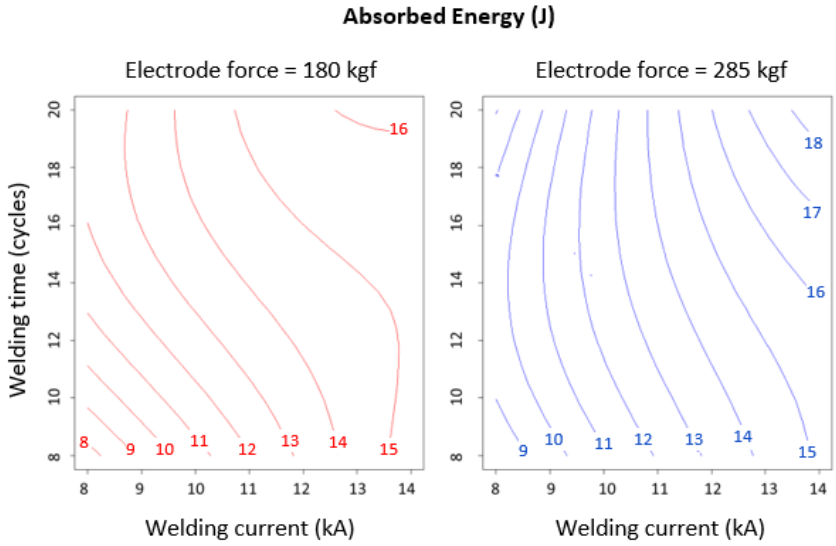

Figure 10 – Contour curves of the response of the Energy Absorbed linear model (J).

3.2 Energy Consumption

The guarantee of structural integrity is linked to the use of electricity. Thus, there is a need to understand how process parameters interact with energy consumption. Hence, it is possible to elaborate strategies that make it possible to reach a compromise relationship between quality and consumption. Figure 11 shows the effect of the experimental factors on Energy Consumption (W). It is observed that both the welding current and time are very influential on energy consumption, unlike electrode force. In this way, the energy consumption analysis is focused on the welding current and time, the interaction between them is shown in Figure 12.

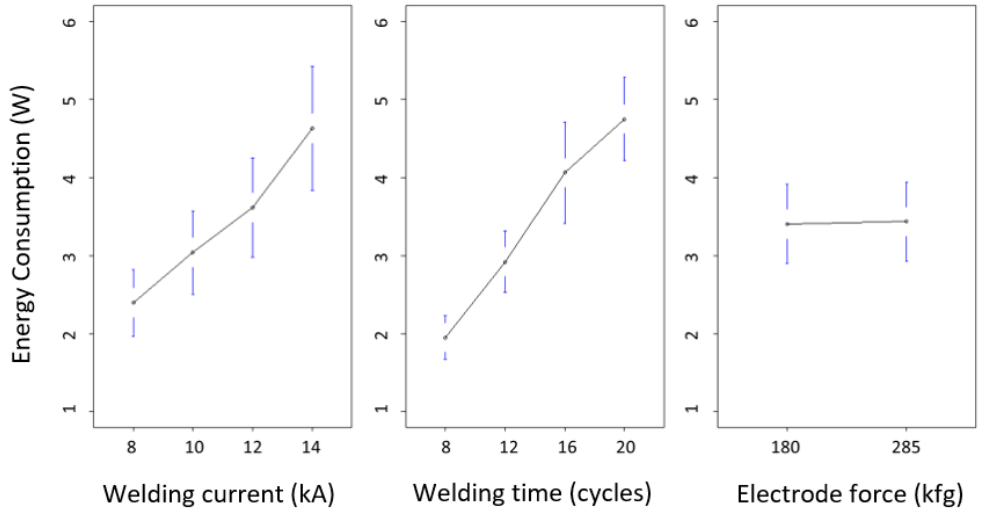

Figure 11 – Effect of factors on energy consumption (W).

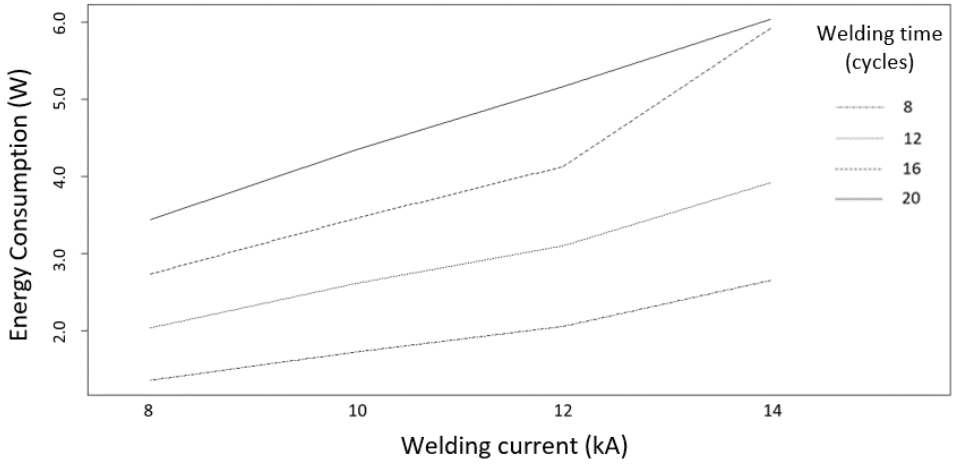

Figure 12 – Effect of the interaction between current and welding time on Energy Consumption (W).

It was not possible to perform the ANOVA considering the interactions since the number of degrees of freedom was insufficient. However, the existence of an interaction between current and time is suspected due to the nature of Joule's Law (Equation 1). Even so, it shows up in the ANOVA only for the main factors. The analysis shows that welding current and time are very influential on consumption. Both factors resulted in a 99.9% confidence interval. Electrode force had no contribution. The residual analysis for the developed model was conducted. The normal distribution exhibited a linear trend and the dispersion, and the p-value given by the Shapiro Wilk test was 0.1159. As the minimum criterion for the p-value is 0.05, this proves that there are no systematic errors.

Thus, a linear experimental model that characterizes the experiment is proposed. This one contemplates how energy consumption is affected by current and time. The result is shown in Figure 13.

```
lm.default(formula = ENER1 ~ I(A^2 * B))

Residuals:
     Min       1Q   Median       3Q      Max
-0.80899 -0.27191  0.00598  0.31481  0.74577

Coefficients:
             Estimate Std. Error t value Pr(>|t|)
(Intercept) 8.809e-01  1.128e-01   7.807 8.57e-11 ***
I(A^2 * B)  1.440e-03  5.673e-05  25.383  < 2e-16 ***
---
Signif. codes:  0 '***' 0.001 '**' 0.01 '*' 0.05 '.' 0.1 ' ' 1

Residual standard error: 0.4169 on 62 degrees of freedom
Multiple R-squared:  0.9122,    Adjusted R-squared:  0.9108
F-statistic: 644.3 on 1 and 62 DF,  p-value: < 2.2e-16
```

Figure 13 – Proposed linear model for Energy Consumption (W).

The model was based on Joule's Law, which expresses the heat equation for spot welding. This resulted in a linear model with a strong correlation, $R^2 = 0.91$. The result indicates the interaction between the two factors, despite the insufficiency of degrees of freedom for ANOVA. The residual analysis of the linear model was also satisfactory. The p-value by the Shapiro Wilk test was 0.138, above the minimum significance of 0.05. The plotted response surface and the contour lines are shown, respectively, in Figures 14 and 15.

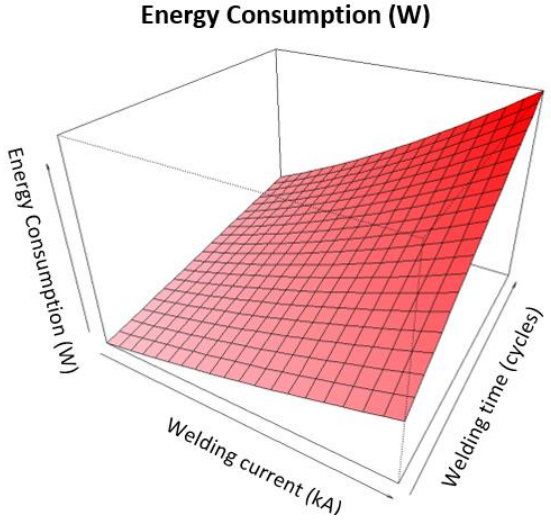

Figure 14 – Response surface for the linear model of Energy Consumption (W).

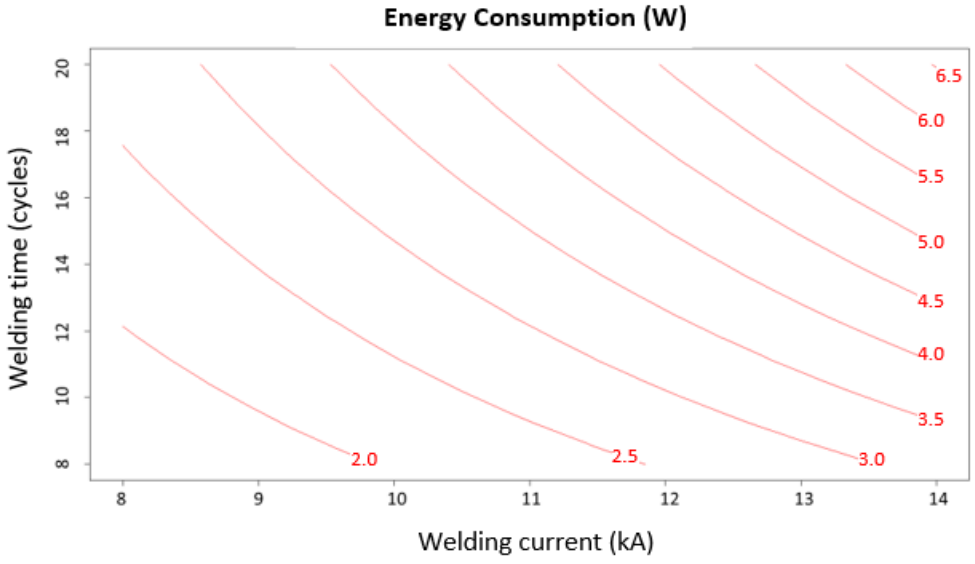

Figure 15 – Contour curves of the response of the linear model of Energy Consumption (W).

Maximum power consumption occurs at maximum current and time values. The result shows that the energy consumed in the welding process is increased by the action of time. Energy consumption is less affected, even with a high magnitude of electrical current, if it flows for a short time.

3.3 Discussion

The analysis shows how the transformation of electrical energy into heat impacts aspects of mechanical performance and energy consumption. Predominantly, the most important factors were current and time. They showed different behaviors regarding the mechanical and energetic responses.

The first analysis indicated the possibility of working on aspects of resistance, by treating the factors disconnectedly. It was also observed the existence of an interaction between current and force. From this, effects are attributed to the resistance to electric current, which constitutes a part of the heat generation. The results showed that greater amounts of heat in the system lead to better F_{max} and En_{abs}.

From an energetic point of view, welding current and time were the most important factors. The lack of more degrees of freedom made it impossible to assess the interaction between the factors by ANOVA. However, phenomenological evidence (Joule effect) and the proposed experimental adjustment indicated a strong interaction between these two factors. Thus, it was found that consumption is strongly influenced by the simultaneous action of current and time.

The industrial scenario is very neglectful of the quality treatment linked to energy consumption. Therefore, the experimental results presented can contribute to reducing operating costs and waste. It was possible to assess that changes only in welding current, or only in time, are sufficient for quality control. Above all, without substantially compromising energy consumption.

4. CONCLUSIONS

This study evaluated the influence of spot-welding parameterization by quality and energy approaches. The experimental analysis included samples with two CR4 steel sheets with 0.7 mm thickness. Electric current, welding time, and electrode force levels were chosen to represent industrial practice. ANOVA was used to evaluate how these process parameters affect the tensile-shear test and the energy consumption. From this it was possible to conclude:

- The joint's mechanical performance characteristics were heavily influenced by current and time. The interaction between current and electrode force is also relevant, but with less significance. The force application changes the interfacial contact between the metal sheets, hence there is an alteration in material resistance. These results are consistent with were found in the literature;
- Energy consumption was affected by electrical current, time, and the interaction of these factors. The interaction is justified by phenomenological observations (Joule's Law) and by the experimental adjustment since there were not enough degrees of freedom for ANOVA. Were not found in literature similar analysis;
- To correct process deviations that affect quality the best alternative is to deal with current and time individually;
- On the other hand, significant reductions in energy consumption are possible with simultaneous changes in welding current and time.

5. REFERENCES

Afshari, Davood. Mechanical properties of resistance spot welds in lightweight applications. 2013. Thesis (Doctorate in Aeronautical and Vehicle Engineering) - KTH Royal Institute of Technology, Stockholm, 2013.

Afshari, D. et al. On residual stresses in resistance spot welded aluminium alloy 6061-T6: Experimental and numerical analysis. Journal of Materials Engineering and Performance, v. 22, n. 12, p. 3612–3619, 2013.

Boersch, I., Füssel, U., Gresch, C., Groβmann, C., Data mining in resistance spot welding. The International Journal of Advanced Manufacturing Technology, Vol. 99, No. 5–8, pp. 1085–1099., 2018

Colombo, T. C. A., Sena, F. M., Faria, J. J. R., Faria, A. R., Analysis Of The Effect Of Spot Welding Current On The Mechanical Behavior And Failure Modes Of Automotive Steel Sheets. In: Proceedings of the 24th International Congress of Mechanical Engineering - COBEM 2017. Curitiba, Brasil., 2017.

International Organization of Motors Vehicle Manufacturers. 2021 Production statistics Paris: OICA, 2021. Disponível em: https://www.oica.net/category/production-statistics/2020-statistics/. Acesso em: 18 jun. 2021.

Kianersi, D.; Mostafaei, A.; Ali, A. Resistance spot welding joints of aisi 316l austenitic stainless steel sheets : phase transformations, mechanical properties and microstructure characterizations. Materials&Design, v. 61, p. 251–263, 2014.

Moshayedi, H; Sattari-Far, I. Resistance spot welding and the effects of welding time and current on residual stresses. Journal of Materials Processing Technology, v. 214, n. 11, p. 2545–2552, 2014.

Nie, X. et al. Optimization of resistance spot welding parameters based on load of welding spot. Hanjie Xuebao/Transactions of the China Welding Institution, v. 39, n. 5, p. 114–120, 2018

Pouranvari, M. Fracture toughness of martensitic stainless steel resistance spot welds. Materials Science and Engineering A, v. 680, p. 97–107, 2017.

Pouranvari, M. et al. Effect of weld nugget size on overload failure mode of resistance spot welds. Science and Technology of Welding and Joining, v. 12, p. 217–225, 2007.

Pouranvari, M.; Marashi, S.P.H. Failure mode transition in AHSS resistance spot welds. Part I. Controlling factors. Materials Science and Engineering A, v. 528, p. 8337–8343, 2011.

Rao, S. S. et al. Resistance spot welding of galvannealed high strength interstitial free steel. Journal of Materials Processing Technology, v. 246, p. 252–261, 2017.

Montgomery, D. C. Design and Analysis of Experiments. 8 ed. John Wiley & Sons Inc., 2012.

Sun, H.T. et al. Effect of variable electrode force on weld quality in resistance spot welding. Science and Technology of Welding and Joining, v. 12, n. 8, p. 718–724, 2007.

Uilj, N. J. D., 2015. Resistance Spot Welding of Advanced High Strength Steels. Ph.D. thesis, Delfit Technische Universiteit, Delfit, Netherlands.

Venugopal, D.; Das, M.; Fernandez, V. Study and implementation of a force stepper and a part fit-up solver algorithm for a servo controlled MFDC spot welder. Proceedings of 2009 IEEE International Conference on Electro/Information Technology, EIT 2009, p. 286–291, 2009.

Williams, N. T. and Parker, J. D., Review of resistance spot welding of steel sheets Part 1: Modelling and control of weld nugget formation. International Materials Reviews, Vol. 49, No. 2, pp. 45-75, 2004.

Yuan, X. et al. Resistance spot welding of dissimilar DP600 and DC54D steels. Journal of Materials Processing Technology, v. 239, p. 31–41, 2017.

Zhang, H.; Senkara, J. Resistance Welding - Fundamentals and applications. [s.l.]. Taylor & Francis, 2006.

6. RESPONSIBILITY NOTICE

The authors are the only responsible for the printed material included in this paper.